Journal of Intelligent & Fuzzy Systems 29 (2015) 2619–2627
DOI:10.3233/IFS-151965
IOS Press

Hybrid velocity switching and fuzzy logic control scheme for cable tunnel inspection robot

Hua Wu[a,*], Yan-Xiong Wu[b], Ling-Zhi Meng[c], Chang-An Liu[a] and Guo-Tian Yang[a]
[a]*School of Control and Computer Engineering, North China Electric Power University, Beijing, P.R. China*
[b]*Department of Disaster Prevention Apparatus, Institute of Disaster Prevention, Hebei, P.R. China*
[c]*State Grid Electric Power Research Institute Beijing Kedong Corporation, P.R. China*

Abstract. This paper describes a hybrid anti-swing control scheme of an inspection robot in tunnels for power transmission cables. The hybrid control scheme consists of velocity switching and fuzzy logic control, so that the robot can be operated smoothly without causing excessive swings in acceleration or deceleration motion. In order to ensure control system robustness for greatest movement in the tunnel, fuzzy logic control is used for horizontal anti-swing control. Velocity switching is adopted for incline anti-swing control, in order to obtain sufficient damping as well as a fast response. The stability of the hybrid system has been analyzed. The experimental results present the practicability and effectiveness of the proposed method.

Keywords: Tunnel inspection robot, anti-swing, hybrid control, fuzzy logic, velocity switching

1. Introduction

At present, electric power cable tunnels have been built under the city for cost-effective transmission, as shown in Fig. 1(a). However, inspection becomes dangerous, because the temperature, toxic gas, insects and high-voltage cables threaten the safety of workers. Therefore, a tunnel inspection robot should meet the needs of good mobility and high reliability for working in such conditions.

There are several types of robots that have been applied to tunnel inspection [7–9, 11] Montero et al. [16] surveyed most tunnel inspection robots. The main drawback is that the workers are required to be in the same location as the robot and a tunnel must be closed for inspection. However, the proposed inspection robot system is mounted on the tracks in the cable tunnel, which allows the robot to work autonomously without closing the cable tunnel.

In this paper, the unprecedented inspection robot is developed as shown in Fig. 1(b). The robot is equipped with several cameras to perform visual environmental monitoring and recognition in the cable tunnel. Meanwhile, wireless communication facilities, gas and smoke sensors are adopted.

The robot is hung on the tracks and driven by one motor. Thus, the locomotion causes the robot to swing during movement. Due to the negative effects induced by the swing motion, this paper focuses on solving the swing problem using hybrid control.

This paper proposes the method to control the robot in order to allow it to move smoothly without excessive swing during acceleration or deceleration. The controller must be designed to overcome residual oscillation caused by accelerated or decelerated mot-ion. Moreover, the incline movement procedure is more

*Corresponding author. Hua Wu, School of Control and Computer Engineering, North China Electric Power University, Beijing, P.R. China. Tel.: +86 13693597566; Fax: +86 010 61772753; E-mail: wishsand@gmail.com.

(a) (b)

Fig. 1. (a) Underground cable tunnel; (b) the cable tunnel inspection robot system.

difficult to control, so that the controller requires the sufficient damping of the load swing and a fast response time. Therefore, the anti-swing control scheme is divided into two parts: horizontal anti-swing control and incline anti-swing control.

Since the swing of the load depends on the acceleration of the motor, many researchers have concentrated on generating reference trajectories to minimize the swing angle. These trajectories are typically obtained by using optimization techniques or input shaping. This consists of a sequence of acceleration and deceleration pulses which are generated so that there is no residual swing [16]. However, given that the high requirement of anti-interference for an inspection robot working in a complex environment, those controller studies are open-loop, which is sensitive to external disturbances and parameter variations and, as a result, did not meet system requirements for this robot. Moreover, this process usually requires a zero-swing angle at the beginning of the process, which is not feasible in practice. Alternatively, closed-loop control is less sensitive to disturbances and parameter variations, thus many researchers have investigated anti-swing control through feedback [6, 13, 22]. Ridout proposed a controller which feeds back the load position and the load swing angle [3]. The feedback gains are calculated by trial and error, which makes the process cumbersome for a wide range of operating conditions. Chung Choo Chung et al. proposed a nonlinear controller to regulate the swinging energy of the pendulum for a cart and pendulum system [4]. The controller is usually designed to achieve the two tasks. The first task is a tracking controller designed to make the controlled plan follow a reference trajectory [14, 21]. The second task is an anti-swing controller [2, 23]. The tracking controller can be obtained from optimal open-loop techniques or input shaping techniques [10]. Also, it can consist of either a proportional-derivative controller [5], or a fuzzy logic controller [1]. Castillo et al. described the application of Ant Colony Optimization (ACO) and Particle Swarm Optimization (PSO) for the optimization of a fuzzy logic controller [15]. Precup et al., proposed an improved fuzzy control system using iterative feedback tuning (IFT) [17]. Similarly, the anti-swing controller is developed according to different methods. Masoud used delayed-position feedback [25], whereas M.A. Ahmad used FLC [12]. The closed-loop control methods are roughly divided into two categories: conventional control schemes and intelligent control schemes. While the inspection robot system is nonlinear and uncertain, an accurate mathematical model cannot be obtained directly. Therefore, the intelligent control schemes such as fuzzy logic control which fit take uncertainty account are ideal, but these schemes can only solve the horizontal anti-swing control problem, and are not suitable to address the incline anti-swing control problem.

To solve the horizontal anti-swing and incline anti-swing problems, fuzzy logic control is adopted to eliminate the swing angle and ensure system robustness. While the requirement for torque in incline movement is given, the velocity switching control [20] is used during incline movement, providing sufficient damping and a fast response time [24]. In this paper, the hybrid velocity switching and fuzzy logic control schemes have been researched to increase the robustness of control and improve system performance.

2. Dynamics of the robot systems

The model of the inspection robot considered in this paper is shown in Fig. 2, where x, θ, F and f represent the robot position, swing angle, driving force and friction, respectively; and M and m represent the mass of the robot and the load, respectively. The length of the link bar is l meters.

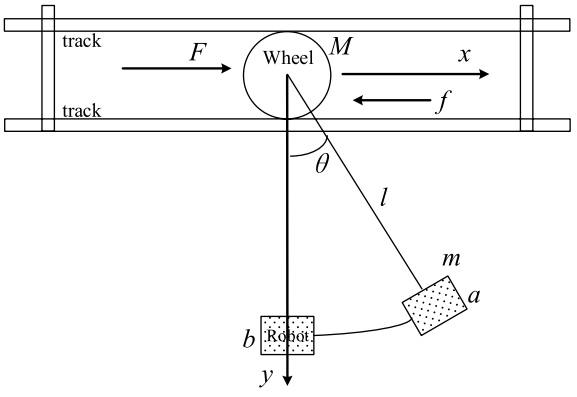

Fig. 2. The model of cable tunnel inspecting robot systems.

The mass and stiffness of cantilever are neglected; thus, the robot and load can be considered as point masses and are assumed to move in a two-dimensional, x-y plane. The coordinates of the trolley and load are (x_M, y_M) and (x_m, y_m).

$$\begin{cases} x_M = x \\ x_m = x + l\sin\theta \\ y_m = l\cos\theta \end{cases} \tag{1}$$

The kinetic energy of the system can be formulated as follows:

$$T = \frac{1}{2}(M+m)\dot{x}^2 + \frac{1}{2}m(\dot{l}^2 + l^2\dot{\theta}^2 + 2\dot{x}\dot{l}\sin\theta + 2\dot{x}\dot{l}\cos\theta) \tag{2}$$

The potential energy is represented as follows:

$$V = mgy_m = mgl(1-\cos\theta) \tag{3}$$

The Lagrangian function L=T-V is expressed as follows:

$$L = \frac{1}{2}M\dot{x}^2 + mgl\cos\theta + \frac{1}{2}m(\dot{x}^2 + \dot{l}^2 + l^2\dot{\theta}^2 + 2\dot{x}\dot{l}\sin\theta + 2\dot{x}l\dot{\theta}\cos\theta) \tag{4}$$

The dynamic system model can be obtained as follows:

$$\begin{cases} (M+m)\ddot{x} + ml\ddot{\theta}\cos\theta - ml\dot{\theta}^2\sin\theta + \mu\dot{x} = F \\ l\ddot{\theta} + \ddot{x}\cos\theta + g\sin\theta = 0 \end{cases} \tag{5}$$

Assume that $\cos\theta = 1$, $\sin\theta = 0$ when θ is small, and that:

$$\ddot{\theta}\cos\theta - \dot{\theta}^2\sin\theta = \frac{d}{dt}(\dot{\theta}\cos\theta) = \frac{d}{dt}(\dot{\theta}) = \ddot{\theta} \tag{6}$$

Equation (5) can be simplified as follows:

$$\begin{cases} (M+m)\ddot{x} + ml\ddot{\theta} + \mu\dot{x} = F \\ l\ddot{\theta} + \ddot{x} + g\theta = 0 \end{cases} \tag{7}$$

Let $x_1 = \dot{x}$, $x_2 = \theta$, $x_3 = \dot{\theta}$. Then, the state space expression can be obtained as follows:

$$\begin{cases} \dot{x}_1 = -\frac{\mu}{M}x_1 + \frac{mg}{M}x_2 + \frac{1}{M}F \\ \dot{x}_2 = x_3 \\ \dot{x}_3 = \frac{\mu}{Ml}x_1 - \frac{(M+m)g}{Ml}x_2 + \frac{1}{Ml}F \end{cases} \tag{8}$$

3. Hybrid control scheme design

In this section, an anti-swing hybrid control scheme will be designed. Velocity switching and fuzzy logic control are employed to address incline swing and horizontal swing problems, respectively. Both will then be extended into a hybrid control scheme with rigid switching conditions between the horizontal and incline movement.

3.1. Fuzzy logic controller

In this paper, an accepted velocity trajectory is used as a reference trajectory, and a velocity-track fuzzy controller is designed. A sub-block diagram of a fuzzy logic controller is shown in Fig. 3, in which $r(t)$ is the velocity reference trajectory; $x(t)$ represents the horizontal position of the robot; θ is the swing angle; and k_1, k_2, k_3 and k_4 are scaling factors for three inputs and one output of the fuzzy logic controller.

Triangular membership functions are chosen for the derivative of the robot position error, swing angle, the derivative of the swing angle and force input. A normalized universe of discourse is used for the three inputs and one output of the fuzzy logic controller. Scaling factors k_1, k_2 and k_3 are chosen to convert the three inputs of the system and activate the rule base effectively, while k_4 is selected to activate the system to generate the desired output. To simplify a rule base, the derivative of robot position error, swing angle, the derivative of swing angle and force are partitioned into five primary fuzzy sets as follows:

Robot position error derivative = {NM NS ZE PS PM}

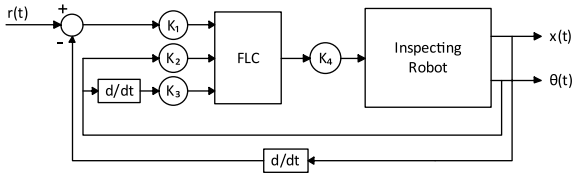

Fig. 3. Fuzzy logic control structure.

Awing angle = {NM NS ZE PS PM}
Awing angle derivative = {NM NS ZE PS PM}
Force = {NM NS ZE PS PM}

The fuzzy logic controller was designed with 30 rules as a closed-loop control strategy for suppressing the swing effect during horizontal movement. The control rules are shown in Table 1. The control surface is shown in Fig. 4.

3.2. Velocity switching control

While the requirement for torque during incline movement is given, the velocity switching control is adopted during incline movement. The velocity switching control features sufficient damping and a fast response time, so that the swing angle can be eliminated quickly. Therefore, this ensures the safety of the robot while crawling up the incline. In the constant-velocity zone, the swing angle is a cosine wave; the value of A can be easily calculated according to the following steps.

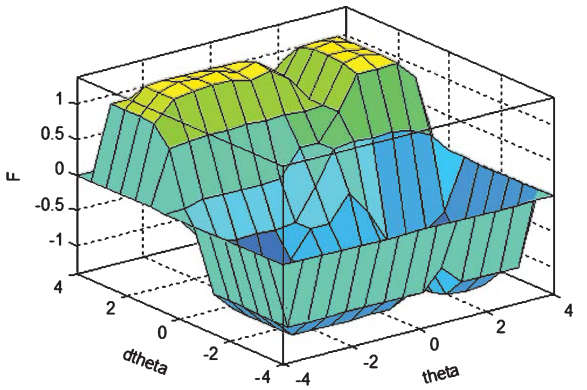

Fig. 4. Control surface.

Table 1
Control rules

F		NB	NS	ZE	PS	PB
dΔx		NB	NS	ZE	PS	PB
F		θ				
	NB	NS	ZE	PS	PB	
dθ	NB	NB	NB	NB	NS	NB
	NS	NB	NS	NS	NS	NB
	ZE	NS	NS	ZE	PS	PS
	PS	PS	PS	PS	PS	PB
	PB	PB	PB	PB	PS	PB

Taking any two time values t_1 and t_2, that the following can be obtained:

$$\begin{cases} \theta(t_1) - \theta(t_2) = 2A \sin\left(\dfrac{\alpha+\beta}{2}\right) \sin\left(\dfrac{\alpha-\beta}{2}\right) \\ \theta(t_1) + \theta(t_2) = 2A \cos\left(\dfrac{\alpha+\beta}{2}\right) \cos\left(\dfrac{\alpha-\beta}{2}\right) \end{cases} \tag{9}$$

where $\alpha = \omega_1 + \phi_0$, $\beta = \omega_2 + \phi_0$.

Since $\sin^2((\alpha+\beta)/2) + \cos^2((\alpha+\beta)/2) = 1$,

$$A = \frac{1}{2}\left[\frac{(\theta(t_1) - \theta(t_2))^2}{\sin^2(-\omega T/2)} + \frac{(\theta(t_1) + \theta(t_2))^2}{\cos^2(-\omega T/2)}\right]^{1/2} \tag{10}$$

where $T = t_2 - t_1$ is the sampling period, $\omega = \omega_n\sqrt{1-\delta^2}$, and the damping of the load δ can be neglected in the modeling of the system, the frequency for the model is $\omega = \omega_n = \sqrt{g/l}$. In this experiment, the filter and sampling module are used to calculate the amplitude A.

Switching from $v0$ to the revised velocity v_x eliminates the swing angle when the load reaches the lowest point (Fig. 2). If the direction of the robot and load are identical, the revised velocity will be $v_0 + v$, where v represents the velocity increment. If the direction of the robot and load are different, the velocity increment will be $v_0 - v$. The velocity switching control does force the swing angle to tend toward zero.

The velocity increment v must be calculated. When the load reaches the highest point, the potential energy of the load is mgl (1-cos$A$). When the load reaches the lowest point, according to conservation of energy:

$$mv^2 \Big/ 2 = mgl(l - \cos A)$$

Thus, the increment velocity v is expressed as:

$$v = \sqrt{2gl(1 - \cos A)}$$

3.3. Hybrid control scheme

Both control approaches described above will be extended into a hybrid control scheme. The model of the inspection robot system is divided into two parts: the continuous part and the discrete part. The continuous part consists of the horizontal movement and incline movement, while the discrete part consists of switching conditions. A model of the hybrid system is shown in Fig. 5.

The horizontal or incline movement subsystem will alternate under switching conditions. The amplitude of swing is chosen as the switching condition variable.

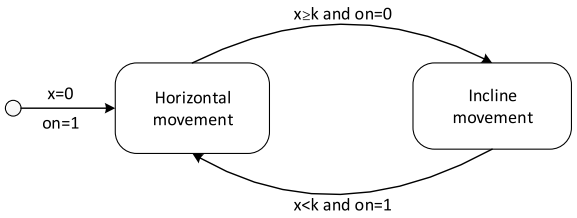

Fig. 5. The model of hybrid system.

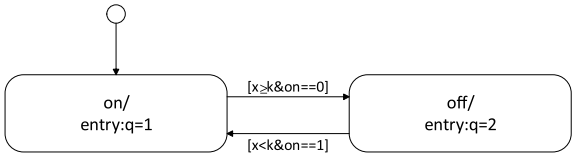

Fig. 6. Stateflow design diagram.

The turning point of the amplitude k is obtained off-line through experiments. The obtained state flow diagram is shown in Fig. 6.

The discrete variable on and continuous variable × (meaning A) codetermine the switching point. When $x \geq k$ and on = 0, it transitions from horizontal movement to incline movement; when $x < k$ and on = 1, it transits from incline movement to horizontal movement.

3.4. Stability of the hybrid control system

In the discussion of the stability of a hybrid control system, a definition of stability must first be introduced. A hybrid control system is stable if hybrid control primitives and deliberative logic will satisfy the following conditions:

- A continuous state within each mode is stable in the sense of the Lyapunov relative to an equilibrium point.
- The mechanism of mode transition is such that when a transition takes place to some mode q_i, its associated states are within the region belonging to q_i.
- The hybrid state remains bounded away from the forbidden regions while the system remains in any particular mode.

The schemes developed for mode sequencing are used to ensure that the 2nd condition holds; there are no restrictions on hybrid flow during transitions, for the modes have no such forbidden regions. Therefore only the 1st condition must be proved for the hybrid system.

To satisfy the 1st condition, it is sufficient to realize that the problem is to verify whether the control primitive u_q is appropriate to meet the control objective and stabilization. A Lyapunov stability argument is used to meet this condition. To facilitate the discussion, The Lyapunov-like function is defined below.

Definition 3.1. (Lyapunv-like function). A Lyapunov-like function for a hybrid system and equilibrium point $\overline{x} \in \Omega_q \subset R^n$ is a real-valued function $V_q(x)$ defined over the region Ω_q, satisfying two conditions:

- Positive definiteness: $V_q(\overline{x}) = 0$ and $V_q(x) > 0$ for $\overline{x} \neq x \in \Omega_q$;
- Negative semi-definite first derivative: for $x \in \Omega_i$

$$\dot{V}_q(x) = \vec{\nabla} V_q(x) f_q(x) \leq 0 \tag{11}$$

To meet the 1st condition, it is sufficient that such a $V_q(x)$ exists for each mode under the action of the control primitive u_q.

With the equilibrium point at the zero-swing angle location, the Lyapunov candidate function is expressed as follows:

$$V(x) = \frac{A}{2}\left(x_1^2 + x_2^2 + x_3^2\right), \ A > 0 \tag{12}$$

$V(0) = 0, \ x \neq 0 \Rightarrow V(x) > 0, \ V(x) > 0, \ V(x) \to \infty$ as $\| x \| \to \infty$

Equation (12) can be used to analyze all vector fields for this problem by appropriately changing the value of the constant A.

Now, regarding system states:

$$\begin{aligned}\dot{V}(x) &= A\left[x_1\dot{x}_1 + x_2\dot{x}_2 + x_3\dot{x}_3\right] \\ &= A\left[-\frac{\mu}{M}x_1^2 + \frac{mg}{M}x_1x_2 + \frac{1}{M}Fx_1 + x_2x_3\right. \\ &\quad \left. + \frac{\mu}{Ml}x_1x_3 - \frac{(M+m)g}{Ml}x_2x_3 + \frac{1}{Ml}Fx_3\right] \\ &= A\left[-0.08x_1^2 + 20x_1x_2 + 0.4Fx_1 - 29x_2x_3\right. \\ &\quad \left. + 0.08x_1x_3 + 0.4Fx_3\right] \end{aligned} \tag{13}$$

gives a general form for the derivative of the Lyapunov function. The objective is to ensure that u_1 and u_2 are specified so that $\dot{V}(x) \leq 0$ for each mode. $\dot{V}(x)$ will be computed and discussed for each mode; $A > 0$ in all cases.

- Mode 1: Horizontal movement

During horizontal movement, the specified control u_1 is used as shown in Fig. 8. The curve of x_1, x_2, and

x_3 can also be obtained from Fig. 8 so that the result is as follows:

$$\dot{V}(x) = A[-0.08x_1^2 + 20x_1x_2 + 0.4Fx_1 + x_2x_3 + 0.08x_1x_3 - 30x_2x_3 + 0.4Fx_3] < 0 \quad (14)$$

The primitive guarantees the robot moves on the horizontal rail without causing excessive swing.

– Mode 2: Incline movement

In this mode, the curve of x_2 indicates that $x_2 > 0$, since $x_1 > 0$, the following is obtained:

$$\dot{V}(x) = A[-0.08x_1^2 + 20x_1x_2 - 29x_2x_3 + 0.08x_1x_3 + 0.4Fx_1 + 0.4Fx_3] < 0 \quad (15)$$

This primitive reduces the swing angle of the robot during incline movement.

Therefore, the stability of the hybrid control system has been verified. The aforementioned discussion verifies the feasibility of the hybrid control system from an analytical perspective. To understand the real response of the system correctly, such technologies must be implemented during test cases that reflect the characteristics of the controllers. The implementation details and some experimental results have been reported below.

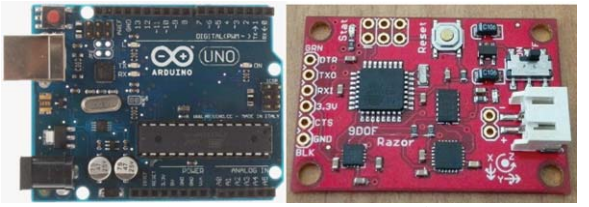

(a) (b)

Fig. 7. Hardware platform and IMU sensor.

4. Experiments

The proposed hybrid control scheme has been implemented on the inspection robot. Redi et al. have implemented an active noise control (ANC) process and algorithm on digital signal processors for real-time experiments in an ANC system [18]. The proposed system was implemented in a cost-effective manner. In order to measure the physical parameters during movement, an incremental encoder mounted behind the servo motor and the 9DoF Razor IMU (shown in Fig. 7(b)) have been adopted. The hybrid controller has been implemented on the Arduino® UNO platform as shown in Fig. 7(a). The data is streamed to a computer with time stamps. The system parameters are as follows: $l = 1.00\,m$, $M = 2.5\,kg$, $m = 5\,kg$, $\mu = 0.2$ and $g = 9.8\,m/s^2$.

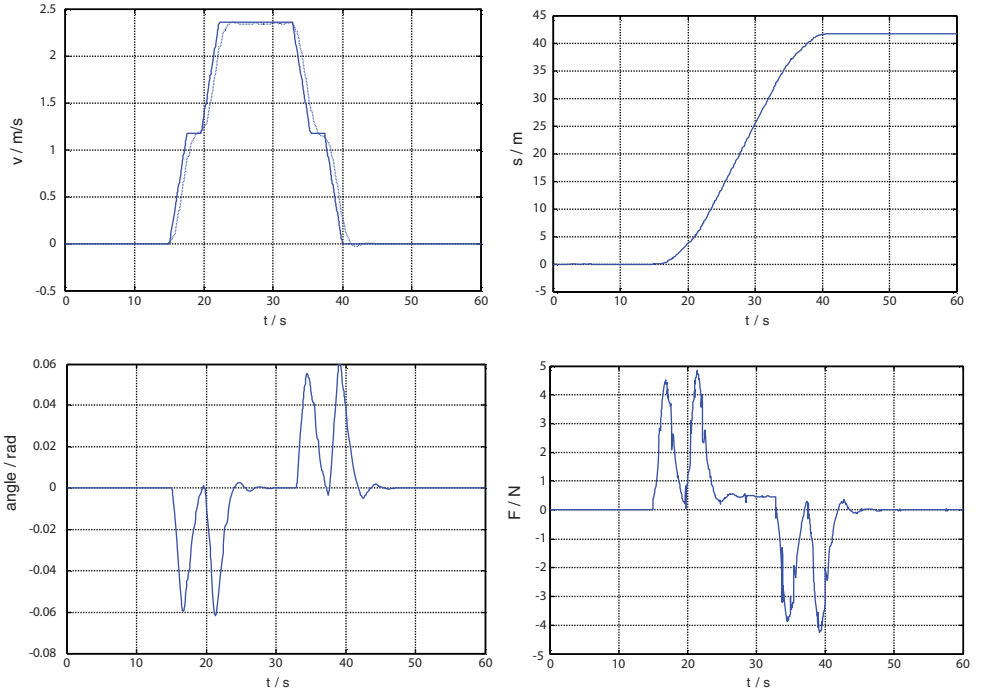

Fig. 8. Response of velocity-track fuzzy control.

An extra velocity trajectory is used as input reference trajectory, shown as a dotted line in Fig. 8. The input tracking capability and swing angle reduction of the velocity-track fuzzy controller are examined. When the robot is running on a horizontal portion of rail, the response of the velocity-track fuzzy control is shown in Fig. 8.

As demonstrated by the figures, the robot velocity closely follows the velocity reference trajectory. The steady-state robot position trajectory of 55 m is achieved within the rise and setting time of 30 s and 40 s, respectively. It is noted from the swing angle response with a maximum residual of ±0.06 rad and after the velocity reference trajectory decrease to 0, that the swing angle stays below 0.002 rad. Therefore, the fuzzy logic controller can eliminate the residual swing angle, and the velocity of the cart tracks the reference trajectory well.

When the robot arrives at the uphill incline portion of the rail, after the acceleration motion of robot, the corresponding response of the velocity switching control is shown in Fig. 9.

The initial swing angle is 0.08 rad, and then it tends toward zero, staying between –0.01 rad and 0.002 rad. The residual angle is effectively eliminated after accelerated motion. This verifies the effectiveness of the velocity switching control during incline movement.

The response of the entire movement process, including the horizontal and incline portions, is shown in Fig. 10.

The robot velocity tracks the velocity reference trajectory well, and the swing angle is eliminated effectively. The input tracking capability of the robot and swing angle reduction have been achieved with a hybrid control scheme, and the proposed hybrid control scheme performs well during the process of movement.

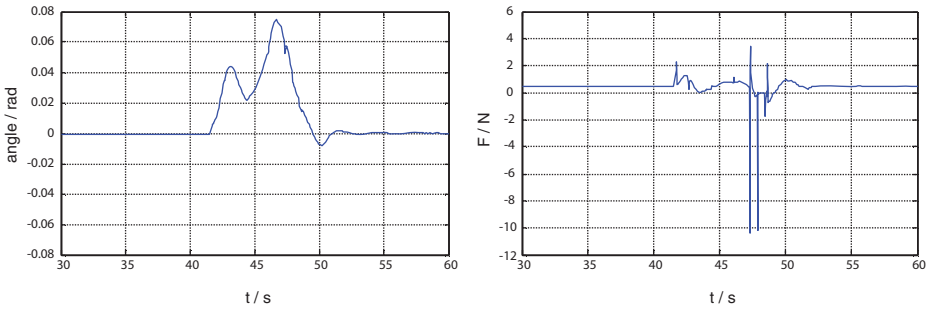

Fig. 9. Response of velocity switching control.

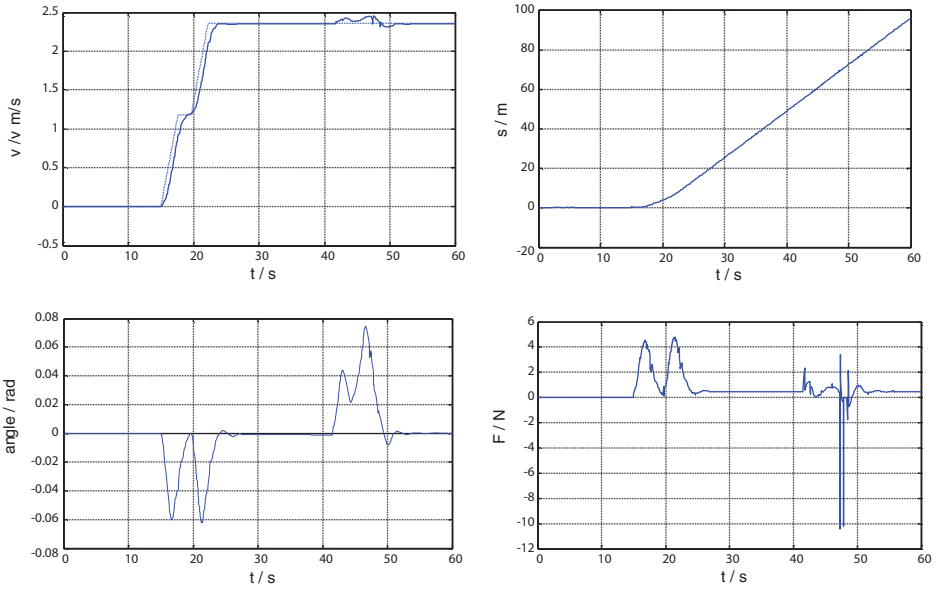

Fig. 10. Response of the horizontal and incline movements.

5. Conclusion

A hybrid velocity switching and fuzzy logic control scheme for a cable tunnel inspection robot is presented. Due to the single wheel structure, the inspection robot can oscillate during the movement process. Therefore, a hybrid control scheme is designed to achieve horizontal anti-swing control and incline anti-swing control. The hybrid control scheme was developed based on fuzzy logic control and velocity switching control, to effectively eliminate horizontal swing and incline swing. Experimental results have verified that effective input tracking capability and swing angle reduction have been achieved with the proposed control scheme.

Acknowledgments

This work is supported by Scientific Research Plan Projects for Higher Schools in Hebei Province (Grant No. QN2015338), the National Natural Science Foundation of China (Grant No. 61105083), Program for New Century Excellent Talents in University (Grant No. NCET-11-0634), the Fundamental Research Funds for the Central Universities (Program No. 12ZX16) and the Program of the Co-Construction with Beijing Municipal of China (Program No. GJ2013005).

References

[1] A.A. Al-Mousa, A.H. Nayfeh and P. Kachroo, Control of rotary cranes using fuzzy logic, *Shock and Vibration* **10** (2003), 81–95.

[2] A. Khatamianfar and A.V. Savkin, A new discrete-time approach to anti-swing tracking control of overhead cranes, in: *Control Applications (CCA), 2014 IEEE Conference on, IEEE, Juan Les Antibes*, 2014, pp. 790–795.

[3] A. Ridout, Anti-swing control of the overhead crane using linear feedback, Journal of Electrical and Electronics Engineering, *Australia* **9** (1989), 17–26.

[4] C.C. Chung and J. Hauser, Nonlinear control of a swinging pendulum, *Automatica* **31** (1995), 851–862.

[5] H.M. Omar *Control of gantry and tower cranes, Ph. D*, Virginia Polytechnic Institute and State University 2003.

[6] H.M. Omar and A.H. Nayfeh, Anti-swing control of gantry and tower cranes using fuzzy and time-delayed feedback with friction compensation, *Shock and Vibration* **12** (2005), 73–89.

[7] J. González, S. Martınez, A. Jardon, and C. Balaguer, Robot-aided tunnel inspection and maintenance system, *Proceedings of the 26th International Symposium on Automation and Robotics in Construction*, Austin, Texas, U.S, 2009, pp. 420–426.

[8] J.G. Victores, S. Martínez, A. Jardón and C. Balaguer, Robot-aided tunnel inspection and maintenance system by vision and proximity sensor integration, *Automation in Construction* **20** (2011), 629–636.

[9] K. Loupos, A. Amditis, C. Stentoumis, P. Chrobocinski, J. Victores, M. Wietek, P. Panetsos, A. Roncaglia, S. Camarinopoulos and V. Kalidromitis *Robotic intelligent vision and control for tunnel inspection and evaluation-The ROBINSPECT EC project, 2014 IEEE International Symposium on Robotic and Sensors Environments (ROSE), IEEE*, Timisoara, Romania, 2014, pp. 72–77

[10] K.L. Sorensen, W. Singhose and S. Dickerson, A controller enabling precise positioning and sway reduction in bridge and gantry cranes, *Control Engineering Practice* **15** (2007), 825–837.

[11] L.S. Liu, A Smart Tunnel Inspection Robot for the Detection of Pipe Culverts, *Applied Mechanics and Materials* **614** (2014), 184–187.

[12] M. Ahmad, N. Hambali, and H. Ishak, Hybrid input shaping and PD-type Fuzzy Logic control scheme of a gantry crane system, Control Applications, *(CCA) & Intelligent Control, (ISIC), 2009 IEEE, IEEE, Saint Petersburg*, 2009, pp. 1051–1056.

[13] M.J. Nalley and M.B. Trabia, Control of overhead cranes using a fuzzy logic controller, *Journal of Intelligent and Fuzzy Systems* **8** (2000), 1–18.

[14] M.E. Serrano, G.J.E. Scaglia, S.A. Godoy, V. Mut and O.A. Ortiz, Trajectory tracking of underactuated surface vessels: A linear algebra approach, Control Systems Technology, *IEEE Transactions on* **22** (2014), 1103–1111.

[15] O. Castillo, R. Martínez-Marroquín, P. Melin, F. Valdez and J. Soria, Comparative study of bio-inspired algorithms applied to the optimization of type-1 and type-2 fuzzy controllers for an autonomous mobile robot, *Information Sciences* **192** (2010), 19–38.

[16] R. Montero, J.G. Victores, S. Martínez, A. Jardón and C. Balaguer, Past, present and future of robotic tunnel inspection, *Automation in Construction* **59** (2015), 99–112.

[17] R.E. Precup, M.L. Tomescu, M.B. R00dac, E.M. Petriu, S. Preitl and C-A Drago06, Iterative performance improvement of fuzzy control systems for three tank systems, *Expert Systems with Applications* **39** (2012), 8288–8299.

[18] R.R. Yacoub, R.T. Bambang, A. Harsoyo and J. Sarwono, DSP Implementation of Combined FIR-Functional Link Neural Network for Active Noise Control, *International Journal of Artificial Intelligence*™ **12** (2014), 36–47.

[19] S. Garrido, M. Abderrahim, A. Giménez, R. Diez and C. Balaguer, Anti-swinging input shaping control of an automatic construction crane, Automation Science and Engineering, *IEEE Transactions on* **5** (2008), 549–557.

[20] T. Anwar and A. Al Juamily, Adaptive Trajectory Control to Achieve Smooth Interaction Force in Robotic Rehabilitation Device, *Procedia Computer Science* **42** (2014), 160–167.

[21] U. Schaper, C. Dittrich, E. Arnold, K. Schneider and O. Sawodny, 2-DOF skew control of boom cranes including state estimation and reference trajectory generation, *Control Engineering Practice* **33** (2014), 63–75.

[22] X. Hao, X. Mei, M. Gajdusek and A.A.H. Damen, Anti-vibration control of contactless planar actuator with manipulator, *International Journal of Applied Electromagnetics and Mechanics* (2008), 311–327.

[23] X. Wu, X. He, N. Sun and Y. Fang, A novel anti-swing control method for 3-d overhead cranes, in: *American Control Conference (ACC), 2014, IEEE*, Portland, OR, 2014, pp. 2821–2826.

[24] X. Xie, J. Li, C.H. Swartz and P. Depriest, Improving Response-Time Performance in Acute Care Delivery: A Systems Approach, *IEEE Transactions on Automation Science & Engineering* **11** (2014), 1240–1249.

[25] Z.N. Masoud and A.H. Nayfeh, Sway reduction on container cranes using delayed feedback controller, *Nonlinear dynamics* **34** (2003), 347–358.